# Laminar Natural Convection of Newtonian and Non – Newtonian Fluids in a Square Enclosure

Ala'a A. Mahdi *      Tahseen Ali Hussian **      Nabeel  Mohammed Jassim*

## Abstract

In this investigation, steady two – dimensional natural convection heat transfer of Newtonian and non-Newtonian fluids inside square enclosure has been analyzed numerically for a wide range of the modified Rayleigh number of ($10^3 \leq Ra \leq 10^5$), with non-dimensional parameter($NE$) of Prandtl – Eyring model ranging from (0 to 10), and modified Prandtl number in the range ($Pr^* =1,10$, and 100). Two types of boundary conditions have been considered. The first,is when the side walls are heated at different uniform temperatures and the horizontal walls are insulated. The second, when the bottom wall is heated by applying a uniform heat flux while the other walls are at the constant cold temperature. Also, the non-Newtonian fluids under consideration were assumed to obey the Prandtl – Eyring model. The numerical results of the values of average Nusselt number have been confirmed by comparing them to similar known yeslts of previous works using the same boundary conditions. Good agreement was obtained. The results are presented in terms of isotherms and streamlines to show the behavior of the fluid flow and temperature fields. In addition, some graphics represent the relation between average Nusselt number and the parameters that are mentioned previously. The results show the effect of non – dimensional parameter ($NE$) on the velocity and temperature profiles. It also shows that the average Nusselt number is a strong function of modified Rayleigh number, modified Prandtl number, non-dimensional parameter, and the boundary conditions. Four different correlations have been made to show the dependence of the average Nusselt number on the non-dimensional parameter, the modified Rayleigh and Prandtl numbers.

**Keywords: Natural Convection – Non-Newtonian Fluids – Square Enclosures - Finite Differences Method.**

الخلاصــــــــة

في هذا البحث، تم إجراء دراسة عددية لانتقال الحرارة بالحمل الطبيعي المستقر ثنائي البعد لموائع نيوتنية وغير – نيوتنية في وسط مغلق مربع الشكل ضمن مدى واسع لعدد رالي المطور ( $10^2 \leq Ra \leq 10^5$ ) وللمقدار اللا بعدي للموديل الرياضي (Prandtl – Eyring) يمتد من ( $0 \leq NE \leq 10$ ) ولعدد براندتل المطور أخذ في المدى ( $Pr^* = 1,10$, and 100 ). افترض نوعان من الظروف الحدية. الأول، عندما تكون الجدران الجانبية مسخنة إلى درجات حرارة مختلفة ومنتظمة والجدران الأفقية معزولة. الثاني، عندما يكون الجدار السفلي مسخن بمصدر حراري ثابت بينما الجدران الأخرى عند درجة حرارة منخفضة وثابتة. كذلك افترض أن سلوك الموائع غير – نيوتنية يخضع للموديل الرياضي (Prandtl – Eyring). لقد تم مقارنة النتائج العددية لمعدل عدد نسلت لهذه الدراسة مع الدراسات السابقة باستعمال نفس الظروف الحدية، ووجد إن الحل العددي الحالي مقارب جداً لهذه البحوث. تم تمثيل نتائج الدراسة بدلالة خطوط درجات الحرارة الثابتة وخطوط الانسياب لبيان سلوك درجة الحرارة والجريان في الحيز. علاوةعلى رسومات بيانية أخرى تمثل علاقة معدل عدد نسلت مع المعاملات المذكورة أعلاه. إن الدراسة الحالية بينت تأثير المقدار اللا بعدي (NE) في السرعة ودرجة الحرارة. كذلك بينت إن عدد نسلت هو دالة قوية من عدد رالي المطور وعدد براندتل المطور والمقدار اللا بعدي (NE) والظروف الحدية. تم إيجاد علاقات تقريبية تمثل اعتما دية معدل عدد نسلت على عدد رالي المطور وعلى عدد براندتل المطور والمقدار اللا بعدي (NE).

## Nomenclature

$NE$ = Fluid index of Prandtl – Eyring model $= \dfrac{\alpha \, B}{L^2}$ .

$A \ \& \ B$ = Fluid consistency indices for the Prandtl – Eyring model ($kg/m.s^2$) & ($s$)

$u$ = Fluid velocity in $x$-direction ($m/s$).

$v$ = Fluid velocity in $y$-direction ($m/s$).

$x \& y$ = Cartesian coordinates.

$P$ = Pressure ($Pa$).

$g$ = Gravitational acceleration ($m/s^2$).

$L$ = Width and Height of enclosure ($m$).

$k$ = Thermal conductivity of fluid ($W/m. \ K$ ).

$q$ = Heat flux ( $W /m^2$ )

$Pr$ = Prandtl number = ($v /\alpha$).

$Pr^*$　= Modified Prandtl number =

$\dfrac{AB}{\rho_o \alpha}$ .

$Ra$　= Modified Rayleigh number

=

$$\begin{cases} Ra_E = \dfrac{\rho_o g\beta L^3 (T_h - T_c)}{AB\alpha} & \text{for B.C.1} \\[3mm] Ra_E^* = Ra_E Nu = \dfrac{\rho_o g\beta L^4 q}{AB\,\alpha k} & \text{for B.C.2} \end{cases}$$

$h$　　　= Heat transfer coefficient ($W$ /$m^2$. $K$ ).

$Nu$　= Nusselt number = $\dfrac{qL}{k(T_h - T_c)}$ .

$Nu_a$ = Average Nusselt number.

$T$　= Temperature ($K$).

$\Delta x \,\&\, \Delta y$ = Grid size in the $x$ and $y$ directions, respectively ($m$).

**Greek Symbols**

$\tau_{yx}$　　=　Shear　stress　($Pa$)

$$= \begin{cases} \mu \dfrac{\partial u}{\partial y} & \text{For Newtonian fluids} \\[3mm] A\sinh^{-1}(B\dfrac{\partial u}{\partial y}) & \text{non-Newt. Fluids} \end{cases}$$

$\tau_{xx}$ = Normal stress in the $x$ direction.

$\tau_{yy}$ = Normal stress in the $y$ direction.

$\rho$　= Density ($kg/m^3$).

$\alpha$　= Thermal diffusivity ($m^2/s$).

$\beta$　= Thermal expansion coefficient

$\psi$　= Stream function ($m^2/s$).

$\omega$　= Vorticity ($1/s$).

$\Delta T$　= Temperature difference ($K$).

$\theta$　= DimensionlessTemperature

$$= \begin{cases} \dfrac{T - T_c}{T_h - T_c} & \text{for B.C.1} \\[3mm] \dfrac{T - T_c}{\dfrac{qL}{k}} & \text{for B.C.2} \end{cases}$$

$\theta_h$　= The dimensionless Temperature of the heated wall.

$\mu$　= Dynamic viscosity, ($kg/m.s$).

$\upsilon$　=　Kinematic viscosity of fluid ($m^2/s$).

## 1. Introduction :-

　　　Natural convection heat transfer of Newtonian and non – Newtonian fluids inside enclosures has been the subject of several studies in the last years. The attention is due to the wide range of applications such as building insulation, solar cavity receivers, ventilation of rooms, storage of grease, mineral oil, or crude oil in containers, nuclear reactor insulation, crystal growth in liquids, and the cooling of electrical components [1]. Natural convection heat transfer in enclosures involves different aspects of problems. This variety of problems comes from possibly geometry characteristic of enclosures, kind of fluid, nature of fluid flow, orientation of the enclosure etc. Most studies on natural convection in enclosures, based on 2D or 3D parallelogram enclosure

investigation, annuli and cylinders with different aspect ratio or diameters, or caliber. It's very interesting because of sensibility of natural convection phenomena from geometry. Also there is, type of fluid with influence on natural convection phenomena [2]. In the present work, a numerical study is performed to analyze the natural convection heat transfer of Newtonian and non – Newtonian fluids inside square enclosure under two different cases of boundary conditions. The fluid motion and heat transfer are affected by modified Rayleigh number, modified Prandtl number, and non – dimensional parameter (*NE*) of Prandtl – Eyring model. The non – dimensional parameter (*NE*) determines the nature of fluid, that is, Newtonian (*NE* = 0) and non – Newtonian fluids (*NE* > 0). The mass, momentum, and energy conservation equations, which are considered to describe the fluid flow and heat transfer for natural convection are nonlinear and because of this non-linearity, some difficulties have arisen in numerical as well as in analytical studies. One of the greatest difficulties with the numerical studies is the problem of divergence of the iterative methods since an analytical solution of the actual problem is extremely

difficult, if not possible, a number of assumptions together with using the computational fluid dynamic techniques are made to obtain approximate results.

## 2 .Mathematical Formulation :-

Consider steady state, two – dimensional, laminar flow of a non – Newtonian fluid with constant physical properties (kinematics viscosity, thermal diffusivity, and thermal expansion coefficient) enclosed in a square enclosure of side length (*L*) under two different cases of thermal boundary conditions, these boundary conditions are:

**Case(I) :-**

The vertical walls are heated to different uniform temperatures ($T_h$ & $T_c$) and the horizontal walls are perfectly insulated (B.C.1), as shown in Fig.(1a).

**Case(II) :-**

The lower wall is heated by applying a uniform heat flux (*q*) and the other walls are isothermally cooled ($T_c$) (B.C.2), as shown inFig.(1b).

Density is also considered as constant value but for buoyant term it's linearised by relation:

$$\rho = \rho_o [1 - \beta (T - T_o)] \qquad (1)$$

where $\beta$ is thermal expansion coefficient for temperature $T_o$.

The governing equations are the following:

$$\frac{\partial u}{\partial x} + \frac{\partial v}{\partial y} = 0 \quad (2)$$

$$\rho_o(u\frac{\partial u}{\partial x} + v\frac{\partial u}{\partial y}) = -\frac{\partial p}{\partial x} + \frac{\partial \tau_{xx}}{\partial x} + \frac{\partial \tau_{yx}}{\partial y} \quad (3)$$

$$\rho_o(u\frac{\partial v}{\partial x} + v\frac{\partial v}{\partial y}) = -\frac{\partial p}{\partial y} + \frac{\partial \tau_{xy}}{\partial x} + \frac{\partial \tau_{yy}}{\partial y} - \rho g \quad (4)$$

$$u\frac{\partial T}{\partial x} + v\frac{\partial T}{\partial y} = \alpha(\frac{\partial^2 T}{\partial x^2} + \frac{\partial^2 T}{\partial y^2}) \quad (5)$$

In the above equations, ($u$, $v$, $\alpha$, $P$, $T$ ) are the fluid velocity components (Fig.1), the thermal diffusivity, the pressure and the temperature. In fact Eqs.(2 to 5) are system of partial differential equations. They are base for natural convection phenomenon for 2D enclosures, presented by mass, momentum and energy conservation equations.

As mentioned in Ref.[3], the Prandtl – Eyring model for non – Newtonian fluids can be represented as:

$$\tau = A \, sinh^{-1}(B\frac{\partial u}{\partial y}) \quad (6)$$

Hence, the shear stresses: are

$$\tau_{xx} = 2A \, sinh^{-1}(B\frac{\partial u}{\partial x}) \quad (7)$$

$$\tau_{yy} = 2A \, sinh^{-1}(B\frac{\partial v}{\partial y}) \quad (8)$$

$$\tau_{xy} = \tau_{yx} = A \, sinh^{-1}[B(\frac{\partial u}{\partial y} + \frac{\partial v}{\partial x})] \quad (9)$$

where $A$ and $B$ are the fluid consistency indices for the Prandtl – Eyring model.

Since it proves to be more convenient to work in terms of a stream function and vorticity, the stream function $\psi(x,y)$ is introduced in the usual manner:

$$u = \frac{\partial \psi}{\partial y} \quad \& \quad v = -\frac{\partial \psi}{\partial x} \quad (10)$$

It is evident from Eq.(10) that the stream function satisfies the continuity equation identically. more Further, for this plane flow field, the only non – zero component of the vorticity is:

$$\omega = \frac{\partial v}{\partial x} - \frac{\partial u}{\partial y}$$

Combining the definition of vorticity and the velocity components in terms of the stream function, and cross – differentiating the Eqs.(3) and (4) reduce the number of equations and eliminate the pressure terms, and substituting for ($\rho$) from Eq.(1), a new set of equations is obtained with independent variables $\psi$, $\omega$ and $T$:

$$\frac{\partial^2 \psi}{\partial x^2} + \frac{\partial^2 \psi}{\partial y^2} = -\omega$$

$$\rho_o[\frac{\partial \psi}{\partial y}\frac{\partial \omega}{\partial x} - \frac{\partial \psi}{\partial x}\frac{\partial \omega}{\partial y}] = AB[\frac{\partial^2 \omega}{\partial x^2} + \frac{\partial^2 \omega}{\partial y^2}] + AB\frac{\partial S_1}{\partial x}$$

$$-\frac{\partial S_2}{\partial y} - 4\frac{\partial S_3}{\partial x}] + S_G$$

$$\frac{\partial \psi}{\partial y}\frac{\partial T}{\partial x}-\frac{\partial \psi}{\partial x}\frac{\partial T}{\partial y}=\alpha(\frac{\partial^2 T}{\partial x^2}+\frac{\partial^2 T}{\partial y^2}) \quad (14)$$

$$S_G = AB[\frac{\partial^4 \psi}{\partial x^4}+\frac{\partial^4 \psi}{\partial y^4}+2\frac{\partial^4 \psi}{\partial x^2 \partial y^2}]+\rho_o g\beta\frac{\partial T}{\partial x} \quad (15)$$

$$S_1 = \frac{\dfrac{\partial^3 \psi}{\partial x \partial y^2}-\dfrac{\partial^3 \psi}{\partial x^3}}{\sqrt{1+(B(\dfrac{\partial^2 \psi}{\partial y^2}-\dfrac{\partial^2 \psi}{\partial x^2}))^2}} \quad , (16a)$$

$$S_2 = \frac{\dfrac{\partial^3 \psi}{\partial y^3}-\dfrac{\partial^3 \psi}{\partial y \partial x^2}}{\sqrt{1+(B(\dfrac{\partial^2 \psi}{\partial y^2}-\dfrac{\partial^2 \psi}{\partial x^2}))^2}} \quad , \& (16b)$$

$$S_3 = \frac{\dfrac{\partial^3 \psi}{\partial x \partial y^2}}{\sqrt{1+(B\dfrac{\partial^2 \psi}{\partial x \partial y})^2}} \quad (16c)$$

Now, the mathematical problem formulated above was placed in dimensionless form by defining the new dimensionless variables [4]:

$$x^* = \frac{x}{L} \quad , \quad y^* = \frac{y}{L}$$

$$\theta = \begin{cases} \dfrac{T-T_c}{T_h-T_c} & \text{for B.C.1} \\[4mm] \dfrac{T-T_c}{\dfrac{qL}{k}} & \text{for B.C.2} \end{cases}$$

$$\psi^* = \frac{\psi}{\alpha} \quad , \quad \omega^* = \frac{\omega L^2}{\alpha}$$

Inserting all the dimensionless variables into Eqs.(12) to (16), yields the following final non – dimensional equations:

$$\frac{\partial^2 \psi^*}{\partial x^{*2}}+\frac{\partial^2 \psi^*}{\partial y^{*2}}=-\omega^* \quad (17)$$

$$\frac{\partial \psi^*}{\partial y^*}\frac{\partial \omega^*}{\partial x^*}-\frac{\partial \psi^*}{\partial x^*}\frac{\partial \omega^*}{\partial y^*}=Pr^*[\frac{\partial^2 \omega^*}{\partial x^{*2}}+\frac{\partial^2 \omega^*}{\partial y^{*2}}]$$
$$+Pr^*[\frac{\partial S_1^*}{\partial x^*}-\frac{\partial S_2^*}{\partial y^*}-4\frac{\partial S_3^*}{\partial x^*}]+S_G^* \quad (18)$$

$$\frac{\partial \psi^*}{\partial y^*}\frac{\partial \theta}{\partial x^*}-\frac{\partial \psi^*}{\partial x^*}\frac{\partial \theta}{\partial y^*}=\frac{\partial^2 \theta}{\partial x^{*2}}+\frac{\partial^2 \theta}{\partial y^{*2}} \quad (19)$$

where;

$$S_G^* = Pr^*[\frac{\partial^4 \psi^*}{\partial x^{*4}}+\frac{\partial^4 \psi^*}{\partial y^{*4}}+2\frac{\partial^4 \psi^*}{\partial x^{*2}\partial y^{*2}}]$$
$$+Pr^*Ra\frac{\partial \theta}{\partial x^*} \quad (20)$$

$$S_1^* = \frac{\dfrac{\partial^3 \psi^*}{\partial x^* \partial y^{*2}}-\dfrac{\partial^3 \psi^*}{\partial x^{*3}}}{\sqrt{1+(NE(\dfrac{\partial^2 \psi^*}{\partial y^{*2}}-\dfrac{\partial^2 \psi^*}{\partial x^{*2}}))^2}} \quad (21)$$

$$S_2^* = \frac{\dfrac{\partial^3 \psi^*}{\partial y^{*3}}-\dfrac{\partial^3 \psi^*}{\partial y^* \partial x^{*2}}}{\sqrt{1+(NE(\dfrac{\partial^2 \psi^*}{\partial y^{*2}}-\dfrac{\partial^2 \psi^*}{\partial x^{*2}}))^2}} \quad (22)$$

$$S_3^* = \frac{\dfrac{\partial^3 \psi^*}{\partial x^* \partial y^{*2}}}{\sqrt{1+(NE(\dfrac{\partial^2 \psi^*}{\partial x^* \partial y^*}))^2}} \quad (23)$$

$$Pr^* = \frac{AB}{\rho_o \alpha} \quad \text{is the modified Prandtl}$$

number.

$$Ra = \begin{cases} Ra_E = \dfrac{\rho_o g\beta L^3 (T_h - T_c)}{AB\alpha} \\ \text{is the modified Rayleigh number for B.C.1} \\[3mm] Ra_E^* = Ra_E Nu = \dfrac{\rho_o g\beta L^4 q}{AB\alpha k} \\ \text{is the modified Rayleigh number for B.C.2} \end{cases}$$

$NE = \dfrac{\alpha B}{L^2}$   is the non- dimensional

parameter of Prandtl – Eyring model.

## 3. Numerical Method :-

Numerical methods have been developed to handle problems involving nonlinearities in the describing equations, or complex geometries involving complicated boundary conditions. A finite-difference technique is applied to solve the governing equations. These three equations (Eqs.(17), (18), and (19)) are to be solved in a given region subject to the condition that the values of the stream function, temperature, and the vorticity, or their derivatives, are prescribed on the boundary of the domain. The finite difference approximation of the governing equations is based on dividing the $(0 \le x^* \le 1)$ interval into (m) equal segments separated by (m+1) nodes. Likewise, the ($y^*$) interval was divided into (n) segments. The usual procedure for obtaining the form of partial differential equation with finite-difference method [5] is to approximate all the partial derivatives in the equation by means of their Taylor series expansions.

Eq.(17) can be approximated using central – difference at the representative interior point (i,j), thus, Eq.(17) can be written for regular mesh as:

$$\psi_{i,j}^* = [2(\psi_{i+1,j}^* + \psi_{i-1,j}^*)(\Delta y^2) + 2(\psi_{i,j+1}^* + \psi_{i,j-1}^*)(\Delta x^2) + 2(\Delta x^2)(\Delta y^2)\omega_{i,j}^*]/[4(\Delta y^2) + 4(\Delta x^2)] \qquad (24)$$

Also, a central – difference formulation can be used for Eqs.(18), and (19). But this problem will need to be solved for reasonably high values of modified Rayleigh numbers; it is known that such a formulation may not be satisfactory owing to the loss of diagonal dominance in the sets of difference equations, with resulting difficulties in convergence when using an iterative procedure.

A forward – backward technique can be introduced to maintain the diagonal dominance coefficient of ($\omega_{i,j}$) in Eq.(18) and ($\theta_{i,j}$) in Eq.(19) which determines the main diagonal elements of the resulting linear system; his technique is outlined as follows [6]:

Set;      $\gamma = \psi_{i+1,j}^* - \psi_{i-1,j}^*$          and

$\beta = \psi_{i,j+1}^* - \psi_{i,j-1}^*$       (25)

Then approximate Eq.(18) by:

expressed in the following difference forms:

$$-(2(\Delta y^2) + 2(\Delta x^2))\omega_{i,j}^* + Pr^*((\Delta y^2)(\omega_{i+1,j}^* + \omega_{i-1,j}^*) + (\Delta x^2)(\omega_{i,j+1}^* + \omega_{i,j-1}^*)) + (\Delta x^2)(\Delta y^2)$$

$$[Pr^*(\frac{\partial S_1^*}{\partial x^*} - \frac{\partial S_2^*}{\partial y^*} - 4\frac{\partial S_3^*}{\partial x^*}) + S_G^* + (\frac{\gamma}{2\Delta x^2}\frac{\partial \omega^*}{\partial y^*}$$

$$-\frac{\beta}{2\Delta y^2}\frac{\partial \omega^*}{\partial x^*})] = 0 \qquad (26)$$

and Eq.(19) by:

$$-(2(\Delta y^2) + 2(\Delta x^2))\,\theta_{i,j} + ((\Delta y^2)(\theta_{i+1,j} + \theta_{i-1,j})$$

$$+ (\Delta x^2)(\theta_{i,j+1} + \theta_{i,j-1})) + (\Delta x^2)(\Delta y^2)[\frac{\gamma}{2\Delta x^2}\frac{\partial \theta}{\partial y^*}$$

$$-\frac{\beta}{2\Delta y^2}\frac{\partial \theta}{\partial x^*}] = 0 \qquad (27)$$

Now, if

$$\gamma \geq 0, \quad \frac{\partial f}{\partial y} = \frac{f_{i,j+1} - f_{i,j}}{\Delta y}, \quad (b_1 = 1), \text{ and } (b_2 = 0)$$

$$\gamma < 0, \quad \frac{\partial f}{\partial y} = \frac{f_{i,j} - f_{i,j-1}}{\Delta y_r}, \quad (b_1 = 0), \text{ and } (b_2 = 1)$$

if

$$\beta \geq 0, \quad \frac{\partial f}{\partial x} = \frac{f_{i,j} - f_{i-1,j}}{\Delta x_r}, \quad (a_1 = 1), \text{ and } (a_2 = 0)$$

$$\beta < 0, \quad \frac{\partial f}{\partial x} = \frac{f_{i+1,j} - f_{i,j}}{\Delta x}, \quad (a_1 = 0), \text{ and } (a_2 = 1)$$

To assure the diagonal dominance of the coefficient matrix for $(\omega_{i,j}^*)$ **and** $(\theta_{i,j})$, which depends on the sign of $(\gamma)$ and $(\beta)$, Eqs.(18) and (19) are

(27)

$$\omega_{i,j}^* = [(0.5\gamma b_1(\Delta x)(\Delta y) + Pr^*(\Delta x^2))\omega_{i,j+1}^*$$

$$+ (0.5\beta a_1(\Delta x)(\Delta y) + Pr^*(\Delta y^2))\omega_{i-1,j}^* -$$

$$(0.5\beta a_2(\Delta x)(\Delta y) - Pr^*(\Delta y^2))\omega_{i+1,j}^* - ($$

$$0.5\gamma b_2(\Delta x)(\Delta y) - Pr^*(\Delta x^2))\omega_{i,j-1}^* + Pr^*$$

$$(\Delta x^2)(\Delta y^2)(\frac{S_{1)i+a_2,j}^* - S_{1)i-a_1,j}^*}{(\Delta x)} -$$

$$\frac{S_{2)i,j+b_1}^* - S_{2)i,j-b_2}^*}{(\Delta y)} - 4\frac{S_{3)i+a_2,j}^* - S_{3)i-a_1,j}^*}{(\Delta x)})$$

$$+ S_{G)i,j}^*(\Delta x^2)(\Delta y^2)]/[2(\Delta y^2) + 2(\Delta x^2)$$

$$+ (\Delta x^2)(\Delta y^2)(\frac{\gamma}{2(\Delta x)(\Delta y)^{b_1}(-\Delta y)^{b_2}}$$

$$+ \frac{\beta}{2(\Delta y)(\Delta x)^{a_1}(-\Delta x)^{a_2}})]$$

$$\theta_{i,j} = [(0.5\gamma b_1(\Delta x)(\Delta y) + (\Delta x^2))\theta_{i,j+1} \qquad (28)$$

$$+ (0.5\beta a_1(\Delta x)(\Delta y) + (\Delta y^2))\theta_{i-1,j} - ($$

$$0.5\beta a_2(\Delta x)(\Delta y) - (\Delta y^2))\theta_{i+1,j} - (0.5$$

$$\gamma b_2(\Delta x)(\Delta y) - (\Delta x^2))\theta_{i,j-1}]/[2(\Delta y^2)$$

$$+ 2(\Delta x^2) + (\Delta x^2)(\Delta y^2)($$

$$\frac{\gamma}{2(\Delta x)(\Delta y)^{b_1}(-\Delta y_r)^{b_2}} + \qquad (29)$$

$$\frac{\beta}{2(\Delta y)(\Delta x_r)^{a_1}(-\Delta x)^{a_2}})]$$

An under – relaxation technique can be applied to accelerate the convergence of Eq.(28); the expression is used in this technique presented in the following :

$$\omega_{i,j}^{*k+1} = (1 - Fv)\omega_{i,j}^{*k} + (Fv)\omega_{i,j}^*(computed)$$

Where ($Fv$) is the relaxation factor for the vorticity. The value of this relaxation factor is in the range of (0 to 2).

In order to obtain results of the conservation equations, The above equations (Eqs.(24), (28), and (29)) are subjected to the following boundary conditions [7]:

**Case (I) :**

$0 \leq x^* \leq 1 \qquad y^* = 0$

$\Rightarrow y^* = \dfrac{\partial y^*}{\partial y^*} = 0 \qquad \dfrac{\partial q}{\partial y^*} = 0$

$0 \leq x^* \leq 1 \qquad y^* = 1$

$\Rightarrow y^* = \dfrac{\partial y^*}{\partial y^*} = 0 \qquad \dfrac{\partial q}{\partial y^*} = 0$

$x^* = 0 \qquad 0 \leq y^* \leq 1$

$\Rightarrow y^* = \dfrac{\partial y^*}{\partial x^*} = 0 \qquad q = q_h$

$x^* = 1 \qquad 0 \leq y^* \leq 1$

$\Rightarrow y^* = \dfrac{\partial y^*}{\partial x^*} = 0 \qquad q = q_c$

**Case (II) :-**

$0 \leq x^* \leq 1 \qquad y^* = 0$

$\Rightarrow y^* = \dfrac{\partial y^*}{\partial y^*} = 0 \qquad \dfrac{\partial q}{\partial y^*} + 1 = 0$

$0 \leq x^* \leq 1 \qquad y^* = 1$

$\Rightarrow y^* = \dfrac{\partial y^*}{\partial y^*} = 0 \qquad q = q_c$

$x^* = 0 \qquad 0 \leq y^* \leq 1$

$\Rightarrow y^* = \dfrac{\partial y^*}{\partial x^*} = 0 \qquad q = q_c$

$x^* = 1 \qquad 0 \leq y^* \leq 1$

$\Rightarrow y^* = \dfrac{\partial y^*}{\partial x^*} = 0 \qquad q = q_c$

Also, the following finite difference equation for the vorticity at a wall is adopted as the boundary condition for the vorticity equation:

$$\omega_o = \frac{3(\psi_o - \psi_1)}{\Delta n^2} - \frac{\omega_1}{2} \qquad \text{where,}$$

$\Delta n = \Delta y$ or $\Delta x$

The physical quantities of interest in this problem are the local Nusselt number along the heated wall [8], defined by:

$$Nu = \frac{qL}{k(T_h - T_c)} \qquad (31)$$

and also the average Nusselt number, which is defined as:

**Case (I) :-**

$$Nu_a = \int_0^1 \frac{\partial \theta}{\partial x^*}\bigg|_{x^* = 0 \text{ or } 1} dy \qquad (32)$$

**Case (II) :-**

$$Nu_a = \int_0^1 \frac{1}{\theta_h} dx \qquad (33)$$

The numerical work starts with giving the distributions of stream function and temperature for natural convection as the zeroth-order approximation. Then, obtain the zeroth-order approximation of vorticity: no flow and pure conduction. Based on these old fields, equation (24) is used to determine point-by-point the new ($y^*$) field, and equation (28) is used to determine the new ($w^*$), while the energy equation (29) is used to determine the new ($\theta$) field. The iteration process is terminated under the following condition:

$$\sum_{i,J}\left|t^{r+1}{}_{i,j}-t^{r}{}_{i,j}\right|\Big/\sum_{i,J}t^{r+1}{}_{i,j}\leq10^{-5}$$

($r$) denotes the iteration step.

where,($\tau$) stands for ($y^*,w^*,$ or $q$);

either

Before starting the computational solution, the grid independence of the results must be tested. Thus, numerical experiments have been carried out to solve a two – dimensional convection problem in which the non – dimensional parameter ($NE = 0$). The modified Prandtl number in this test is set to be (6.7), while the grid size varies from ($10\times10$) to ($60\times60$) for different values of modified Rayleigh number as shown in Fig.(2). It is found that the change in the Nusselt number for grid size of ($35\times35$) and ($45\times45$) is less than (0.8) percent for the range of modified Rayleigh number ($10^3\leq Ra_E\leq10^5$). Therefore, the number of grid that is adopted in the present study is ($35\times35$) for both two cases. The number of grid point was selected as a compromise between accuracy and speed of computation.

#### 4. Results and Discussion :-

**Case (I) :-** Square enclosure under B.C.1

*a-Temperature and Flow Fields:*

The contour lines of the temperature distribution and flow fields for different values of system parameters are presented in Figs.(3) to (6). In this case, the energy is transported from hot wall to cold wall by conduction (i.e. $Nu_a=1$) at modified Rayleigh number and

non – dimensional parameter (*NE*) are less than ($10^3$) and (1) respectively. In the conduction regime, the isotherms are almost parallel to isothermal walls. As $Ra_E$ or *NE* increases, a circulatory motion is established because of the buoyancy effects. The flow consists of a single cell filling the entire enclosure and rotating slowly in the clockwise direction. Initially, the convection cell show a diagonal symmetry about the two central lines of enclosure, and, it has a maximum value for the stream function ($\psi_{max}=1.549$) at $Ra_E=100, Pr^*=1,$ and $NE=10$. The small value of $\psi_{max}$ characterizes a very weak convective flow. However, an increase in $Ra_E$ or *NE* results in an asymmetric flow pattern producing closer streamlines near the walls, and change the direction of the isotherms, as shown in Figs.(3) and (4). As $Ra_E$ is increased further for a given *NE*, or *NE* is increased for high values of $Ra_E$ , the streamlines more closer to the vertical walls, producing strong boundary layer effects on the isothermal walls. As a result, the stratified region become bigger, as shown in Figs.(5) and (6). Although the flow remains unicellular at all modified Rayleigh numbers and non- dimensional parameters (*NE*), the velocity in the upper right corner and lower left corner increases substantially.

Fig.(7) represent the variation of stream function with modified Rayleigh number compared for different values of non – dimensional parameter and modified Prandtl number (*Pr\**=10). At

low Rayleigh ($Ra_E < 10^3$), $\psi$ seems to be invariable with $Pr^*$ and $NE$ (i.e. at $NE < 1$), this is due to dominance of conduction as mentioned before. At higher $Ra_E$, the stream function ($\psi$) increases with increasing $Pr^*$ or $NE$, and reaches a stationary value for $NE \geq 1$, at $Ra_E \geq 10^4$. It is also seen that the value of $\psi_{max}$ increases and reaches the peak value at $Ra_E = 10^5$, for $Pr^* = 100$ and $NE = 1$. It is also show that the peak value of $\psi_{max}$ depends on $Ra_E$ and $NE$ at a fixed $Pr^*$.

Fig.(5a) shows the streamlines at $Ra_E = 10^5$, $Pr^* = 1$ and $NE = 0$. This flow consists of one large cell rotating in the enclosure. It also shows the flow rising in a layer near the heated wall, turning the corner at the top of the enclosure, moving adjacent the insulated wall, and flowing downward in a layer near the cooled wall. It also indicates the flow has a maximum value for the stream function ($\psi_{max}= 11.24$). This case has been studied by many investigators [9 to 11] for a square enclosure filled with a Newtonian fluid ($NE = 0$), and serves as a base case.

b-*Heat Transfer Coefficient:*

To understand the heat transfer process by natural convection, the heat transfer coefficient ($h$), must be to evaluated but to make the present work have generality, the calculated results must be in dimensionless form. Therefore, one must be needed to evaluate Nusselt number ($Nu$) as a function of influence parameters. Fig.(8) shows the variation in average Nusselt number versus modified

Rayleigh number with different values of non – dimensional parameter and modified Prandtl number ($Pr^*$=10) on the hot wall of the enclosure. It is clear that $Nu_a$ equal to one in the conduction regime. The reason is that the viscous force is greater than the buoyancy force therefore the heat is transported by conduction. It is also seen that for range of modified Rayleigh number before ($10^3$), the rate of increase in $Nu_a$ against $Ra_E$ for different values of $NE$ and a fixed $Pr^*$ is relatively small. But, $Nu_a$ increases rapidly as $NE$ increases for $Ra_E \geq 10^3$ expressing the increase in convective heat transfer. It is also noticed that the effect of $NE$ on $Nu_a$ is more pronounced as the $Ra_E$ numbers increase.

**Case (II) :-** Square enclosure under B.C.2
a-*Temperature and Flow Fields:*

Figs.(9) to (14) show the contour lines of the temperature distribution and flow fields for the present case.

A change in boundary conditions from (Case (I)) to (Case (II)), modifies the temperature and velocity fields significantly. Initially (i.e. at $Ra_E^* = 10$) the flow consists of a single cell filling the entire enclosure and rotating slowly in the clockwise direction. However, an increase in $Ra_E^*$ or $NE$ results in changing the flow pattern from unicellular to multicellular flow. Fig.(13c) shows the streamlines at $Ra_E^* = 10^5$, $NE = 0.1$, and $Pr^* = 10$. This

flow exhibits two counter – rotating cells, each covering half of the enclosure. Both components have the same maximum magnitude ($\psi_{max}$ = 24.36), but are of opposite sign indicaties an opposite direction of flow. These two cells are symmetric about the center line of the enclosure. The convective velocity near the wall is lower than that along the line of symmetry. It also indicates the flow rising slightly in the middle, turning at the top of the enclosure, moving adjacent the cold wall, turning, and falling down the vertical cold wall.

As $Ra_E^*$ or *NE* increases more the streamlines moves closer toward the line of symmetry, producing a strong boundary layer effects on the middle region of the enclosure, and increase the convective velocity in the upper and lower middle region of the enclosure as shown in Figs.(9) and (11). Fig.(15) represent the variation of $\psi$ with $Ra_E^*$ for different values of *NE* and *Pr\**=10.

Furthermore, the isotherms are symmetric about the vertical line at $x = 0.5$ for different values of system parameters, and the maximum temperature $\theta_{max}$ always occurs at the middle of the lower wall, and is a function of $Ra_E^*$, *NE*, and *Pr\**.

Furthermore any increase in $Ra_E^*$ or *NE* causes a high change in temperature field which concentrates in the small region near the top surface as shown in Figs.(10), (12), and (14). The isotherms in the upper region are almost horizontal for

a large portion of the enclosure which allows a large amount of heat to be rejected on the top wall, and gives the vertical walls weaker effects than that in case (I). For a fixed $Ra_E^*$, the amount of energy removed on the top wall is increased with *NE*. Indeed, the large scale modification in the temperature and flow fields due to the change in the boundary conditions from (Case(I)) to (Case (II)) is mostly concentrated in small region, near the top surface. A significant amount of energy is also rejected at the vertical surfaces when the $Ra_E^*$ or *NE* is small. However, the heat transfer on this surfaces decreases with an increase in $Ra_E^*$ or *NE* which clearly implies that the effect of the vertical walls boundary Conditions diminishes with higher velocities or higher $Ra_E^*$.

### b-*Heat Transfer Coefficient*:

The average Nusselt number as defined by Eq.(33) is presented in Fig.(16). It is seen that $Ra_E^*$ and *NE* are less than ($10^4$) and (1) respectively, the rate of increase in $Nu_a$ is relatively small. Then, $Nu_a$ increases rapidly as $Ra_E^*$ or *NE* increases expressing the existence and increase convective heat transfer. As already indicated by the temperature field, the average Nusselt number for the present case is higher than that for the case (I) for the same given condition.

Finally, four correlation equations have been predicted depending on variation in modified Rayleigh number,

modified Prandtl number, and non – dimensional parameter of the Prandtl – Eyring model for both two cases, by using least square method.

**Case (I):** Square enclosure under B.C.1

$$Nu_a = 0.151\, Ra_E^{0.298}\, \text{Pr}^{*\,0.047}\, (NE+\mathbf{1})^{4.78},$$
$$\mathbf{0} \leq NE \leq 0.1, \quad R = 0.9336 \tag{34}$$

and,

$$Nu_a = 0.264\, Ra_E^{0.265}\, \text{Pr}^{*\,0.188}\, (NE+\mathbf{1})^{0.147},$$
$$0.1 < NE, \quad R = 0.9427 \tag{35}$$

**Case (II):** Square enclosure under B.C.2

$$Nu_a = 1.542\, Ra_E^{*\,0.145}\, \text{Pr}^{*\,0.0296}\, (NE+\mathbf{1})^{2.28},$$
$$\mathbf{0} \leq NE \leq 0.1, \quad R = 0.9127 \tag{36}$$

and,

$$Nu_a = 1.475\, Ra_E^{*\,0.163}\, \text{Pr}^{*\,0.102}\, (NE+\mathbf{1})^{0.0611},$$
$$0.1 < NE, \quad R = 0.9491 \tag{37}$$

The above correlations are acceptable in the range of modified Rayleigh number ($10^2$ to $10^5$), modified Prandtl number (1 to 100), and non – dimensional parameter ( $NE$= 0 to 10 ).

To ensure that these approximation correlations are usable, the coefficient of determination ($R$) had been obtained for each equation. The minimum value of ($R$) was (0.874), that means these approximate equations are good for predicting the value of average Nusselt number. Figs.(17) and (18) show the comparison between numerical and predicted results. Agreement between numerical and predicted is close, although most the predicted points lie near the theoretical line.

Further, values of the average Nusselt number along the hot wall of the square enclosure under (B.C.1) at the steady-state flow for ($Ra_E$= $10^3$, $10^4$, $10^5$ and $10^6$) and at modified Prandtl number of ($Pr*$ = 0.71 and 6.7)  are given in Table (1). It is seen again that the present values of ($Nu_a$) are in very good agreement with that obtained by different authors, such as Elba et al.[1]. Subba [9] has analyzed a similar problem for different values of modified Rayleigh numbers. The comparison with his results show agreements within (± 4 %). Subba [9] presented his results in a graph and some errors might have been introduced in reading the graph. Also, as shown in Table (1,b), there are some differences between the present work and those of Hortmann et al.[10] and Davis [11]. These differences are due to the finite difference approximation and the computing system used.

## 5. Conclusions :-

The present numerical solutions for natural convection heat transfer of Newtonian and non-Newtonian fluids for square enclosure under two different cases of boundary conditions (B.C.1 and B.C.2), show that the effects of the enclosure and the type of fluid on the flow development

and the energy transfer are dominant and complex. The main conclusions of the present study are:

1- For the two cases that have been solved, it has been demonstrated that the average Nusselt number  is a strong function of modified Rayleigh number, non – dimensional parameter (*NE*), and modified Prandtl number, also the results show the average Nusselt number:

a- increases as (*Ra*) increases, for a given values of (*NE*) and (*Pr\**).

b- increases as (*NE*) increases except for (*NE* > 0.1) at (*Ra* $\geq 10^5$), for a given value of (*Pr\**).

c- increases as (*Pr\**) increases, for a given values of (*Ra*) and (*NE*).

d- $Nu_a$ for the second case of boundary conditions (B.C.2) is always higher than for the first case (B.C.1).

2- For large modified Rayleigh number, the non – dimensional parameter (*NE*) of the Prandtl – Eyring model has, for a given modified Rayleigh and Prandtl numbers, a large effect on the heat transfer rate. The peak in average Nusselt number occurs between (0.1≤ *NE* ≤10), depending upon modified Rayleigh and Prandtl numbers. As the (*Ra*) increases, the value of non – dimensional parameter at which maximum average Nusselt number takes place shift towards lower values of (*NE*) for all values of (*Pr\**), while for small (*Ra*), it does not have much effect on the heat transfer because in this situation, the convection is very weak and the dominant mode of energy transfer is conduction.

3- For Case(II), The maximum dimensionless temperature is always located at the middle of the bottom wall.

4- In the first case of the boundary conditions (B.C.1), the flow is mainly single cell flow, while in the second case (B.C.2), the flow consists of two counter-rotating cells, each covering half of the enclosure. This flow causes significant increasing in the heat transfer rate  as (*Ra* or *NE*) increases, since it has stronger circulation  warm effects on the fluid motion.

5- The study shows how to predict the effectiveness of a given enclosure in terms of energy transfer or to design an efficient one by suitably selecting the type of fluid or the shape of the enclosure or both.

**References :**

[1] Elba, O. B., Julio, C. R., and Obidio, R., "Numerical Simulation for the Natural Convection Flow", Numerical Methods in Fluids, Vol. 30, PP. 237-254, 2000.

[2] Miomir, R., "Numerical Investigation of Laminar Natural Convection in Inclined Square Enclosures", Physics, Chemistry and Technology, Vol. 2, PP.149-157, 2001.

[3] J. M. Coulson, and J. S. Richardson, "Chemical Engineering", Bergamon, International Library, Vol. 3, 1983.

[4] Myers, E., "Analytical Methods in Conduction Heat Transfer", Mc Graw – Hill Book Company, Inc., 1971.

[5] Bejan, A., "Convection Heat Transfer", Wiley, Inter Science Publication, John Wiley and Sons, Inc., 1984.

[6] Najdat N., "Laminar Flow Separation in Constructed Channel", Ph.D. Thesis, Michigan State University, 1987.

[7] G., Lauriat, "Numerical Study of the Interaction of Natural Convection with Radiation in Nongray Gases in a Narrow Vertical Cavity", Int. Journal of Heat Transfer, Vol. 2, PP. 153-158, 1982.

[8] Frank, K., and Mark, S., "Principles of Heat Transfer", 5th Edition, PWS Publishing Company, 1997.

[9] Subba, R., "Numerical Simulation of Laminar Natural Convection in Shallow Inclined Enclosures", Int. Journal of Heat Transfer, Vol. 2, PP. 263-268, 1982.

[10] M. Hortmann, M. Peric, and G. Scheuerer, "Finite Volume Multi grid Prediction of Laminar Natural Convection: Bench-Mark Solutions", Int. Journal for Numerical Methods in Fluids, Vol. 11, PP. 189-207, 1990.

[11] G., De Vahl, "Natural Convection of Air in a Square Cavity: A Bench Mark Numerical Solution", Int. Journal for Numerical Methods in Fluids, Vol. 3, PP. 249-264, 1983.

**Table (1) Nusselt number comparison for the case of the square enclosure filled with Newtonian fluids and heated from the side.   a- $Pr^*$=0.71,   b- $Pr^*$=6.7**

(a)

| | $Nu_a$ | | | |
|---|---|---|---|---|
| | Hortmann et al. | Davis [11] | Elba et | Present |
| $10^4$ | 2.2436 | 2.234 | 2.2492 | 2.18494 |
| $10^5$ | 4.61653 | 4.487 | 4.5473 | 4.5311 |
| $10^6$ | 9.4216 | 8.81 | 8.7817 | 9.471 |

(b)

| $Ra_E$ | $Nu_a$ | |
|---|---|---|
| | Subba | Present |
| $10^3$ | 1.112 | 1.1149 |
| $10^4$ | 2.252 | 2.2741 |
| $10^5$ | 5.092 | 5.1037 |
| $10^6$ | 11.3697 | 10.915 |



(a)

88

**(b)**
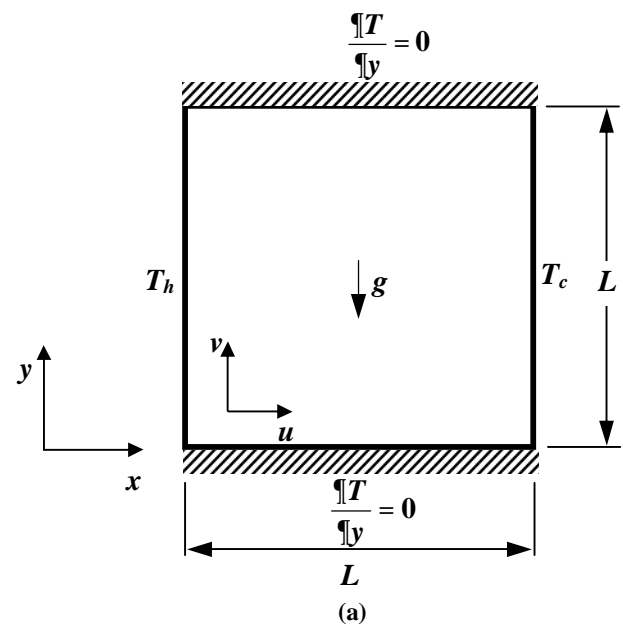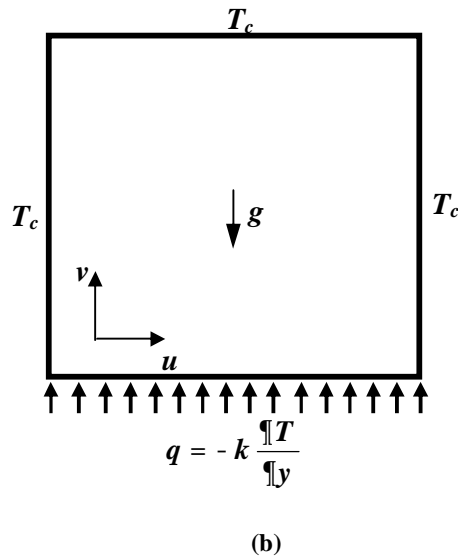
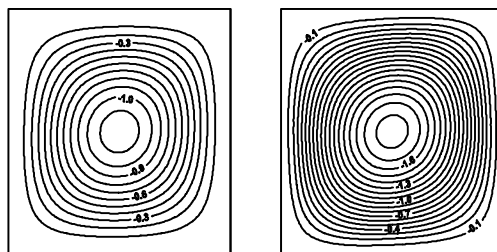**Fig.(1) Physical model and coordinate
system. (a) case (I); (b) case (II)**





**Fig.(3) Pattern of streamlines for $Ra_E = 10^3$
and $Pr^* = 10$. (a) NE=0, (b) NE=0.1, (c) NE=1,
(d) NE=10.　　For Case (I)**
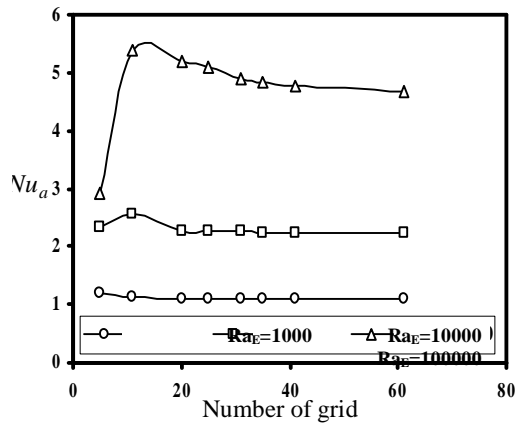


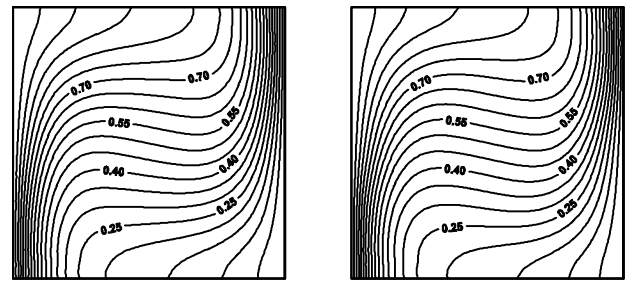**Fig.(2) Variation of Nusselt number
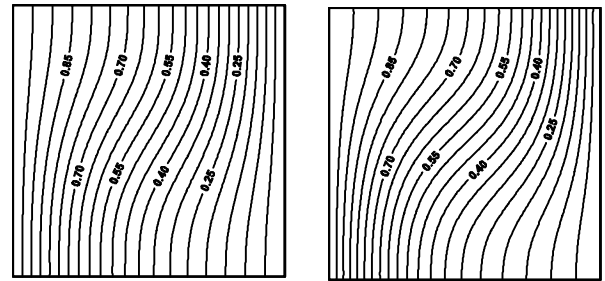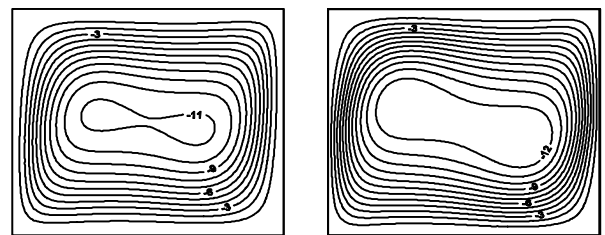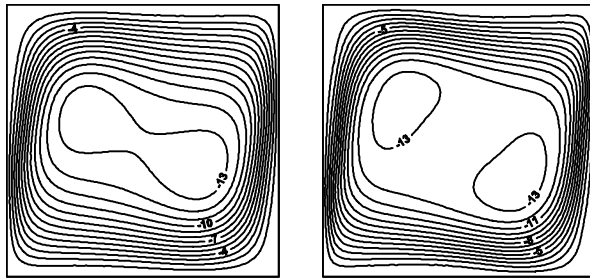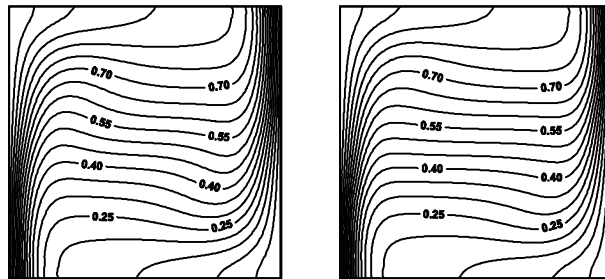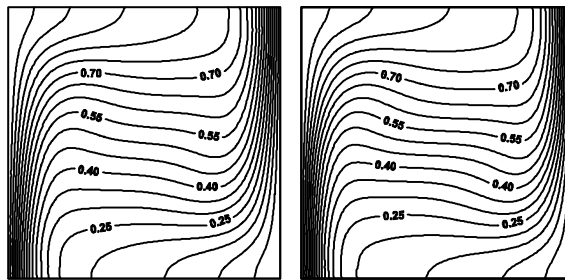with the number of grid points for
different modified Rayleigh
number.　Case (I) .**

**Fig.(4) Pattern of isotherms for $Ra_E = 10^3$
and $Pr^* = 10$. (a) NE=0, (b) NE=0.1, (c) NE=1,
(d) NE=10.　　For Case (I)**



a)　　　　　　　　　　　(b)

(a)　　　　　　　　　　　(b)

(c)                 (d)

**Fig.(5) Pattern of streamlines for $Ra_E = 10^5$
and $Pr^* = 1$. (a) $NE=0$, (b) $NE=0.003$, (c)
$NE=0.01$, (d) $NE=0.1$.     For Case (I)**



(a)                 (b)



(c)                 (d)

**Fig.(6) Pattern of isotherms for $Ra_E = 10^5$
and $Pr^* = 1$. (a) $NE=0$, (b) $NE=0.003$, (c)
$NE=0.01$, (d) $NE=0.1$.     For Case (I)**
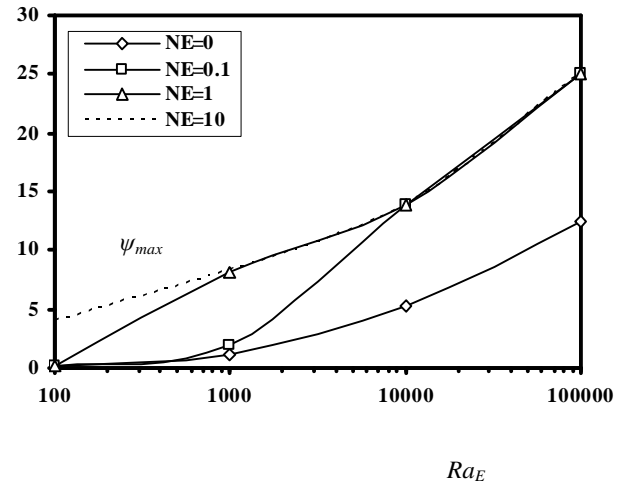


**Fig.(7) Variation in         $(\psi)_{max}$   with
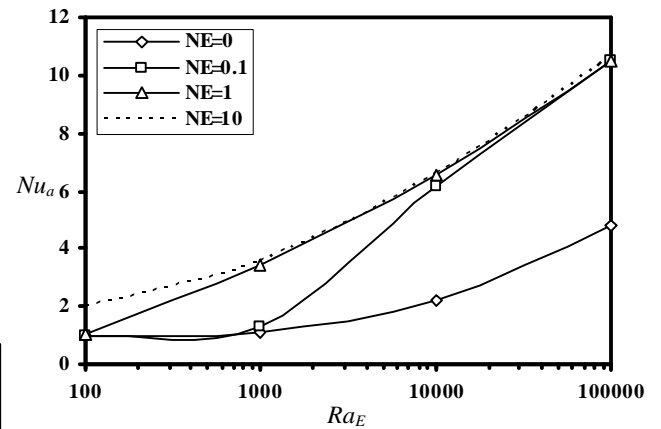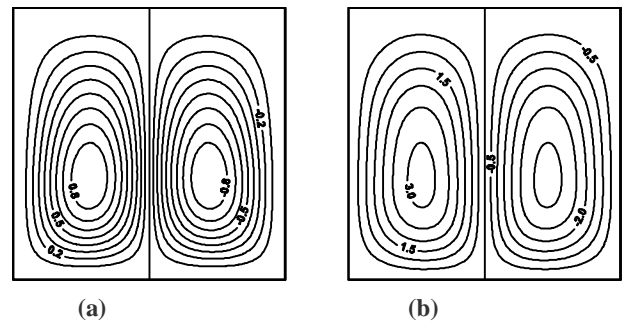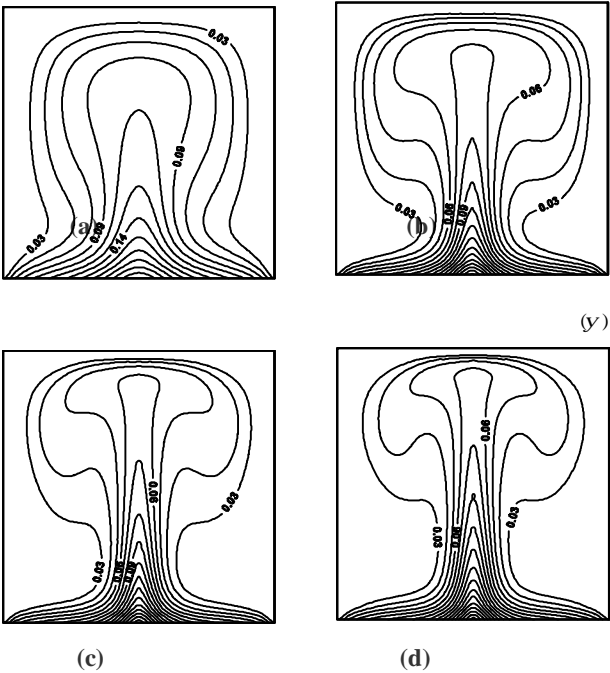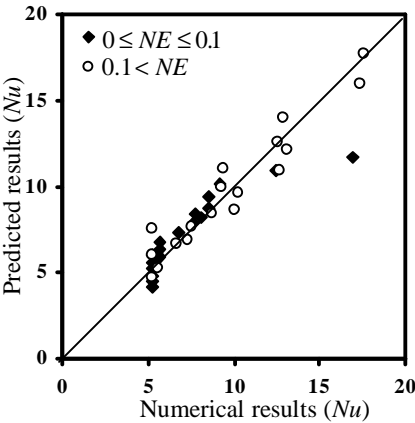the $Ra_E$ for    different values of $NE$ and
$Pr^*=10$.   Case (I)**



**Fig.(8) Variation in $Nu_a$ with the $Ra_E$ for
different values of $NE$ and $Pr^*=10$.
Case(I)**



(a)                              (b)

**Fig.(14) Pattern of isotherms for $Ra^*_E =10^5$ and $Pr^*=10$. (a) $NE$=0, (b) $NE$=0.03, (c) $NE$=0.1,   (d) $NE$=1.     For Case (II)**

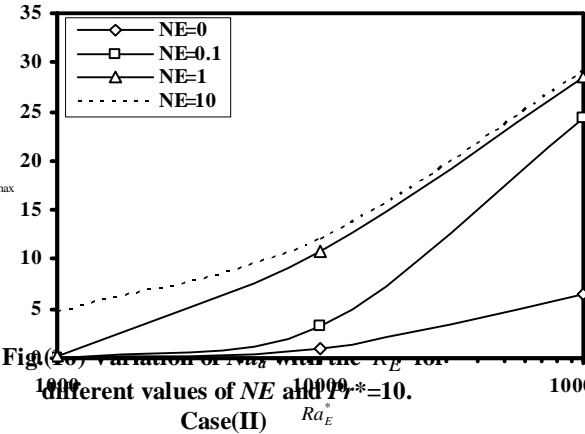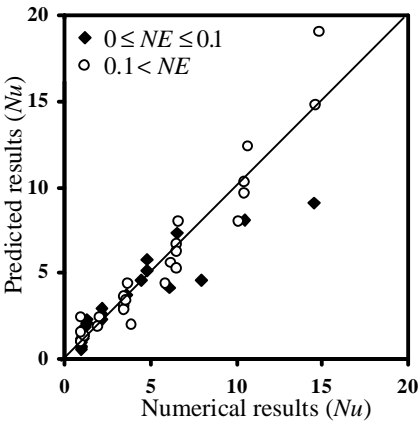**Fig.(17)  Numerical results vs. Predicted results of correlation equation.   Case (I)**

**Fig.(18)  Numerical results vs. Predicted results of correlation equation.   Case (II)**